J Mater Sci (2008) 43:2550–2554
DOI 10.1007/s10853-008-2447-y

Electrochemical corrosion behavior of cast Mg–Al–RE–Mn Alloys in NaCl solution

Ning Liu · Jianli Wang · Yaoming Wu · Limin Wang

Received: 24 March 2007 / Accepted: 4 January 2008 / Published online: 20 February 2008

Abstract The electrochemical corrosion behavior of Mg–6Al–0.4Mn and Mg–6Al–4RE–0.4Mn (RE = Mischmetal) alloys is investigated in 3.5% NaCl solution. The results of corrosion process, polarization behavior, and electrochemical impedance spectroscopy of the alloys reveal that Mg–6Al–4RE–0.4Mn exhibits enhanced corrosion resistance. The addition of RE stabilizes the solid solution and modifies the passive film through a finer microstructure.

Introduction

Magnesium alloys have been increasingly used in automotive, aerospace, and telecommunication industries as structure materials as they exhibit extremely low weight and good workability. However, the inferior corrosion resistance attributed to high chemistry activity of Mg limits their widespread applications [1–4]. When the magnesium alloy is exposed to aggressive electrolyte species such as chloride ions, the corrosion resistance is especially poor. There are two main reasons for the poor corrosion resistance. Firstly, there is internal galvanic corrosion caused by second phases or impurities. Secondly, the passive film is much less stable than that on aluminum. This passivity provides only poor pitting resistance for magnesium alloys [5, 6].

Alloying with other elements is an essential method to enhance corrosion resistance property of magnesium and several alloys with improved corrosion behavior have been developed [7]. Mn is often added to magnesium alloy to improve the corrosion property since it can dramatically reduce the contents of heavy element impurities, especially iron [8]. Currently, Mg–Al base alloys are the most widely used magnesium alloys because they show a good combination of mechanical properties and corrosion resistance. It has been reported that a significant enrichment of the aluminum oxide in the passive film is observed on Mg–Al alloys, especially on alloys containing more than 4% aluminum. This results in increased stability of the passive film and consequently an improved corrosion resistance [9]. Rare earth elements are also beneficial to the corrosion resistance of magnesium alloy [10, 11]. Thus, in this work, the electrochemical corrosion behavior of Mg–Al–RE–Mn alloys in 3.5% NaCl solution is investigated.

Experiment

Mg–6Al–0.4Mn (AM) and Mg–6Al–4RE–0.4Mn (ARM) alloys were prepared by metal mold-casting method. The specimens were polished successively on finer grades of emery papers up to 1,000 grit. Subsequently, samples were cleaned in an ultrasonic bath in distilled water and acetone, and then dried in the warm air. Then they were welded with electrical wire and embedded in epoxy resin as working electrodes for electrochemical measurements. The exposed area was about 1 cm^2. 3.5% NaCl solution was used as corrosive media for the electrochemical measurements. The pH value of the NaCl solution was adjusted to seven

N. Liu · J. Wang · Y. Wu · L. Wang (✉)
Key Laboratory of Rare Earth Chemistry and Physics, Changchun Institute of Applied Chemistry, Chinese Academy of Sciences, Changchun 130022, China
e-mail: lmwang@ciac.jl.cn

N. Liu · J. Wang
Graduate School of the Chinese Academy of Sciences, Beijing 100049, China

using diluted sodium hydroxide. All chemicals in this work were analytical grade. Electrochemical experiments were carried out in the corrosion cell containing 500 ml of electrolyte using a standard three electrode configuration: saturated calomel as the reference, with a platinum thread as the counter, and the working electrode. All experiments were conducted at room temperature without stirring and deaeration.

Open circuit potential test and polarization curves were measured with a CHI 660B electrochemical measurement system. The polarizations started from a cathodic potential and the scanning rate was 10 mVs^{-1}. Electrochemical impedance spectroscopy (EIS) was measured using Solartron 1287 Potentiostat/Galvanostat and a Solartron 1255 frequency response analyzer with Z-POLT software. EIS was recorded at open circuit potentials, in the frequency ranging from 100 kHz to 10 mHz, with a sinusoidal signal perturbation of 10 mV.

Results and discussion

Open circuit potential tests

Figure 1 shows the corrosion potentials of the AM and ARM alloys fluctuating with time while being immersed in the NaCl solution. The corrosion potential of the ARM alloy keeps steady and nearly constant during most of the immersion time. The AM alloy achieves a relatively stable potential in about 5 min, much quicker than the ARM alloy which takes about 1 h, as shown in Fig. 1b. After the initial stage, the corrosion potential of the ARM alloy increases very slowly as compared with that of the AM alloy. After 12 h, the corrosion potential of the AM alloy fluctuates severely, whereas the corrosion potential of the ARM alloy becomes unsteady after 15 h. (The corresponding curves for the severely fluctuated potential in Fig. 1 have been omitted for clarity.)

The dissolution of magnesium begins from the adsorption of hydroxyl ions on the surface and magnesium hydroxide is produced by electrochemical reaction. But chloride ions also adsorb on the film and easily penetrate the hydroxide film and form a basic chloride salt, which is very diffluent in the solution [12]. In the long immersion, the relatively stable potential of the ARM alloy indicates a more effective protection supplied by the film against corrosion attack of the chloride ions.

Electrochemical polarization

The electrochemical polarization curves of the fresh polished AM and ARM alloys are shown in Fig. 2. It can be

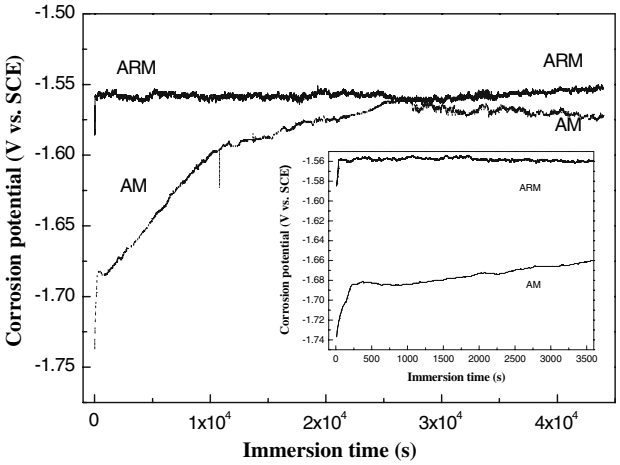

Fig. 1 Variation of corrosion potentials of the AM and ARM alloys immersed in 3.5% NaCl solution. Inset: the corrosion potentials for first hour

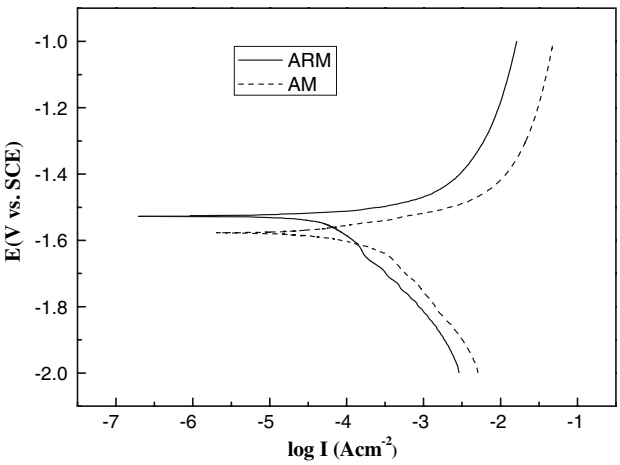

Fig. 2 Polarization curves of the AM and ARM alloys

seen that the addition of RE in the ARM alloy shifts the corrosion potential to more positive values. The shape of the polarization curves is almost the same for the AM and ARM alloys. Much sharper changes are observed in the anodic polarization curve than in the cathodic polarization curve. Generally, the cathodic polarization curves mainly represent the cathodic hydrogen evolution by β-phase, while the anodic ones represent the dissolution of magnesium [13]. According to Fig. 2, in the cathodic parts, the current density of the AM alloy is higher than that of the ARM alloy, it indicates that the cathodic reaction is kinetically easier and has lower overpotential on the AM alloy than on the ARM alloy [14]. In the anodic parts, the ARM alloy has a lower current density and stabilized magnesium dissolution. RE makes α-phase less active in anodic dissolution and stabilizes the solid solution. The decrease of cathodic and anodic current densities is the reason for the decrease for the corrosion density [15].

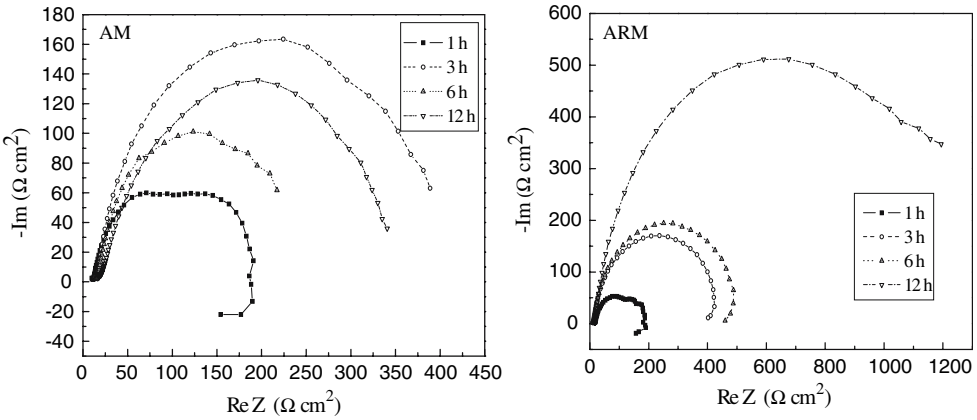

Fig. 3 Electrochemical impedance diagrams obtained at the corrosion potential after different immersion times for the AM and ARM alloys

Electrochemical impedance spectroscopy

Figure 3 shows impedance diagrams obtained at E_{corr} of the AM and ARM alloys for different immersion times in the NaCl solution. For the first hour of immersion for both alloys, the shape of the diagrams is that of a high-frequency capacitive loop followed by a medium capacitive loop and extended by an inductive loop, similar to that obtained for pure magnesium [16]. After 3 h, only single capacitive loops are observed.

According to the previous studies [17, 18], the high-frequency capacitive loop appears to result from both charge transfer and a film effect of corrosion products. The medium-frequency capacitive loop is attributed to relaxation of mass transport in the solid phase due to the growth of the corrosion product layer. The inductive loop may be due to the occurrence of relaxation processes of adsorbed species. Moreover the inductive loop is closely associated with the dependence of the coverage of a protective surface film [19]. The inductive loop disappears after more longer than 1 h, when the protective oxide layer develops and the dissolution rate decreases. Only single capacitive loops are observed after 3 h, which may be related to the fact that the time constants for the surface film and for the electron transfer process are close [20].

As for pure magnesium, the impedance diagram is fitted by an equivalent circuit: a charge-transfer resistance in parallel with the double-layer capacity, and the capacity of the corrosion product layer in parallel with a film resistance. However, for magnesium alloys the fit is not suitable. To improve the fit, the double layer capacity is fixed at a value of 50 μFcm^2. According to this analysis, it is concluded that the resistance associated with the high-frequency part of the diagrams essentially represents the film resistance (R_f) [18]. So Fig. 4 reports the variation of R_f for both the alloys. These values can be used to evaluate the corrosion resistance of the alloys. In the first hour, R_f for the AM alloy is higher, for which the corrosion of the AM alloy takes place more easily

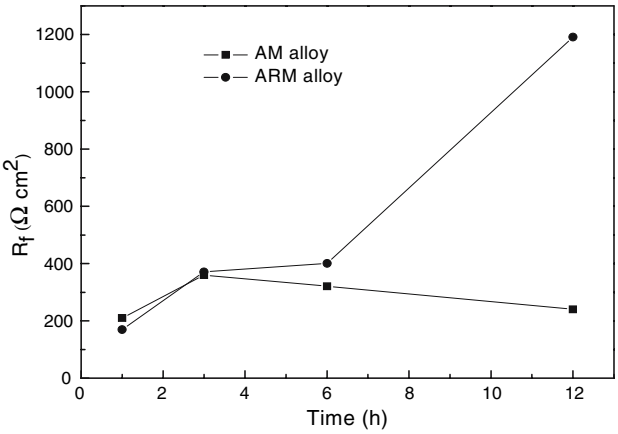

Fig. 4 Variation of R_f versus immersion time for the AM and ARM alloys

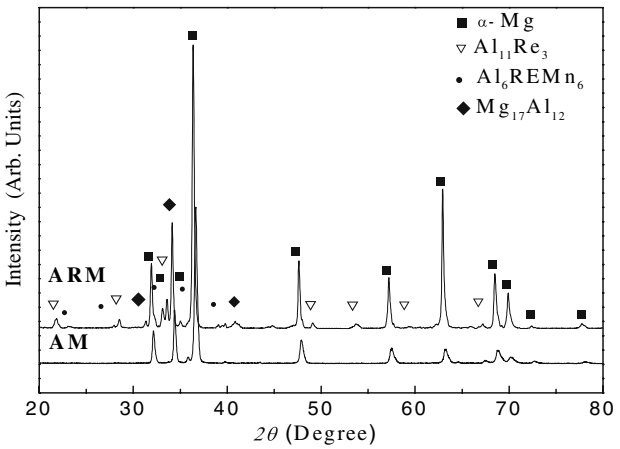

Fig. 5 X-ray diffraction patterns of the AM and ARM alloys

and the protective film forms more quickly than that of the ARM alloy. It is consistent with the results of open circuit potential tests. For long immersion times (3 h, 6 h, 12 h), R_f is higher for the ARM alloy and increases with the immersion time, due to a thickening of the corrosion product layer. However, R_f for the AM alloy changes irregularly, due to poor stability and desquamation film over the exposure time.

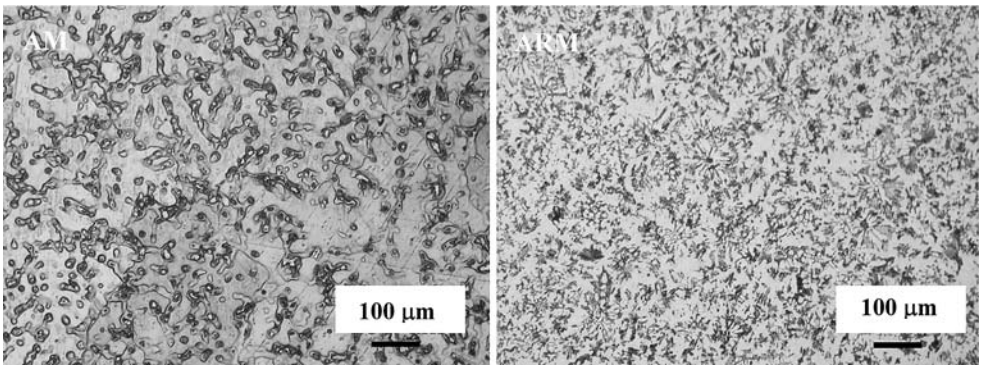

Fig. 6 Optical micrographs of the AM and ARM alloys

It shows an improvement of the corrosion resistance for the RE-containing electrode.

Corrosion morphology and mechanism

The different corrosion behaviors of the AM and ARM alloys can be attributed to differences in their microstructure and composition. Figure 5 shows the XRD patterns of the AM and ARM alloys. It can be seen that the AM alloy is mainly composed of α-Mg and β-$Mg_{17}Al_{12}$ phases. Additional peaks of $Al_{11}RE_3$ and Al_6REMn_6 appear as a result of RE addition. The optical microstructures of the AM and ARM alloys are shown in Fig. 6, which shows that the alloys consist of primary matrix and precipitates. The addition of RE refines the microstructure and forms more continuous β-phase.

After immersion in NaCl solution for 3 h (Fig. 7a, b), the corrosion of the alloys mainly occurs in α-phase grains, while the β-phase particles suffer little attack and clearly stand on the surface. Figure 7c and d shows the corrosion morphologies of both immersion samples for 20 h after removing the corrosion products. The corrosion on the surface of the ARM alloy is uniform and has relatively

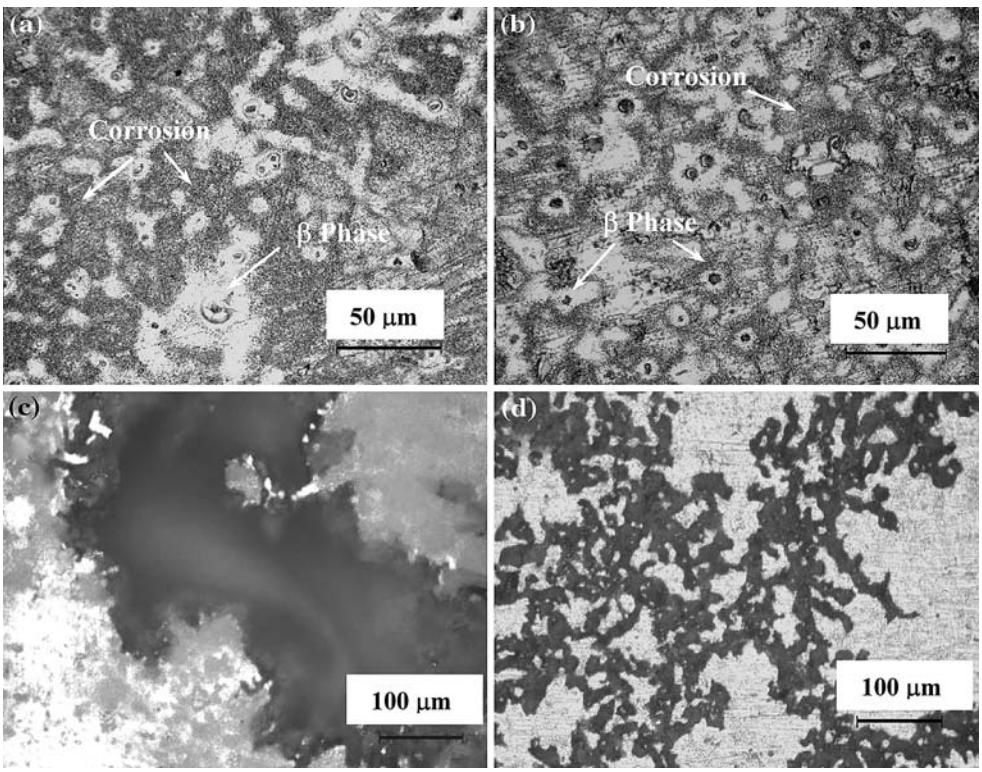

Fig. 7 Optical micrographs of corrosion surface morphology after different immersion time: (**a**) AM alloy after 3 h, (**b**) ARM alloy after 3 h, (**c**) AM alloy after 20 h and (**d**) ARM alloy after 20 h

shallow depth; however, the large and deep pits are on the surface of the AM alloy.

Song et al. [13, 21] proposed that the β-phase could act as either a corrosion barrier or a galvanic cathode accelerating corrosion. The role that dominates the corrosion process depends on the amount and distribution of the β-phase. During the initial period of corrosion, as the corrosion process starts from the α-phase, the β-phase should mainly act as a galvanic cathode. It can be supposed that RE and some intermetallic precipitates, which are originally present as cathodes in galvanic corrosion, are composed of less active cathodes compared to the magnesium anode. The reduced potential difference leads to the slower hydrogen evolution and stabilized magnesium dissolution in aqueous solution. For long immersion times, the continuous β-phase does not easily fall out by undermining when the surrounding α-phase has been preferentially dissolved and forms a more homogeneous oxide film [13, 21]. The addition of RE refines the microstructure, the continuous β-phase delays corrosion developing between grains across the grain boundaries. The incorporation of oxidized RE into the brucite-layered structure modifies the passive film and also reduces breakdown susceptibility of the corrosion film [22, 23].

Conclusions

The electrochemical corrosion behavior of Mg–6Al–0.4Mn and Mg–6Al–4RE–0.4Mn (RE = Mischmetal) alloys in 3.5% NaCl solution is investigated. Mg–6Al–4RE–0.2Mn alloy exhibits enhanced corrosion resistance as compared to Mg–6Al–0.4Mn alloy, and the corrosion potential shifts to more positive values. For Mg–6Al–4RE–0.2Mn alloy, the slower hydrogen evolution and the stabilized magnesium dissolution are attributed to the addition of RE with some intermetallic precipitates. For long immersion times, Mg–6Al–4RE–0.4Mn alloy appears to have a passive film with improved stability and heterogeneity, as supported by the results of electrochemical impedance measurements and open circuit potential with time.

Acknowledgement This work is supported by Chinese Academy of Science for Distinguished Talents Program, and The Science Program of the Promotes Northeast of CAS (KGCX2-SW-216, DBZX-1-001) and Science and Technology Program of Changchun (05GG54).

References

1. Lunder O, Aune TKR, Nisancioglu K (1987) Corros 43:291
2. Nordlien JH, Ono S, Masuko N, Nisancioglu K (1997) Corros Sci 39:1397
3. Gray JE, Luan B (2002) J Alloys Compd 336:88
4. Ambat R, Aung NN, Zhou W (2000) Corros Sci 42:1433
5. Makar GL, Kruger J (1993) Int Mater Rev 38:138
6. Song G, Atrens A (1999) Adv Eng Mater 1:11
7. Rosalbino F, Angelini E, Negri SD, Saccone A, Delfino S (2005) Intermetallics 13:55
8. Pettersen G, Westengen H, Hoier R, Lohne D (1996) Mater Sci Eng A 207:115
9. Nordlien JH, Nisancioglu K, Ono S, Masuko N (1997) J Electrochem Soc 144:461
10. Nakatsugawa I, Kamado S, Kojima Y, Ninomiya R, Kubota K (1998) Corros Rev 16:139
11. Morales ED, Ghali E, Hort N, Dietzel W, Kainer KU (2003) Mater Sci Forum 419–422:867
12. Godard HP, Jepson WB, Bothewell MR, Kane RL (1967) The corrosion of light metals. Wiley, 260 pp
13. Song G, Atrens A (2003) Adv Eng Mater 5:837
14. Chang JW, Guo XC, Fu PH, Peng LM, Ding WJ (2007) Electrochim Acta 52:3160
15. Cao C (1994) Corrosion electrochemical, Chinese society of corrosion and protection of metals, Chemical and Industrial Press, 72 pp
16. Pébère N, Riera C, Dabosi F (1990) Electrochim Acta 35:555
17. Baril G, Pébère N (2001) Corr Sci 43:471
18. Baril G, Blanc C, Pébère N (2001) J Electrochem Soc 148:B489
19. Song G, Atrens A, St John D, Wu X, Nairn J (1997) Corros Sci 39:1981
20. Kumar GG, Munichandraiah N (2001) J Solid State Electrochem 5:8
21. Song G (2005) Adv Eng Mater 7:563
22. Yao HB, Li Y, Wee ATS, Pan JS, Chai JW (2001) Appl Surf Sci 173:54
23. Miller PL, Shaw BA, Wendt RG, Moshier W (1995) Corrosion 51:922